

Characterization of the normal cardiac myofiber field in goat measured with MR-diffusion tensor imaging

L. GEERTS,¹ P. BOVENDEERD,² K. NICOLAY,^{2,3} AND T. ARTS^{1,4}

¹Department of Mechanical Engineering and ²Department of Biomedical Engineering, Eindhoven University of Technology, 5600 MB Eindhoven;

³Department of Experimental In Vivo NMR, Utrecht University, 3508 TC Utrecht;

and ⁴Department of Biophysics, Maastricht University, Maastricht, 6200 MD The Netherlands

Received 5 November 2001; accepted in final form 20 February 2002

Geerts, L., P. Bovendeerd, K. Nicolay, and T. Arts.

Characterization of the normal cardiac myofiber field in goat measured with MR-diffusion tensor imaging. *Am J Physiol Heart Circ Physiol* 283: H139–H145, 2002. First published February 28, 2002; 10.1152/ajpheart.00968.2001.—Cardiac myofiber orientation is a crucial determinant of the distribution of myocardial wall stress. Myofiber orientation is commonly quantified by helix and transverse angles. Accuracy of reported helix angles is limited. Reported transverse angle data are incomplete. We measured cardiac myofiber orientation postmortem in five healthy goat hearts using magnetic resonance-diffusion tensor imaging. A novel local wall-bound coordinate system was derived from the characteristics of the fiber field. The transmural course of the helix angle corresponded to data reported in literature. The mean midwall transverse angle ranged from $-12 \pm 4^\circ$ near the apex to $+9.0 \pm 4^\circ$ near the base of the left ventricle, which is in agreement with the course predicted by Rijcken et al. (18) using a uniform load hypothesis. The divergence of the myofiber field was computed, which is a measure for the extent to which wall stress is transmitted through the myofiber alone. It appeared to be $<0.07 \text{ mm}^{-1}$ throughout the myocardial walls except for the fusion sites between the left and right ventricles and the insertion sites of the papillary muscles.

cardiac myofiber orientation; cardiac coordinate system

WITHIN THE CARDIAC WALL, muscle fibers are oriented in a characteristic helixlike pattern, which is similar across various animal species. Streeter et al. (24, 26) were the first to quantitatively characterize the cardiac myofiber field. Since then, myofiber orientation has been measured by Ross and Streeter (19), Greenbaum et al. (9), and more recently by Nielsen et al. (14). For quantification of fiber orientation, the helix and transverse angle have been introduced by Streeter (23). The helix angle represents the longitudinal component of the fiber orientation, whereas the transverse angle represents the transmural component of the fiber orientation. Measured transmural helix angle courses typically range from $+60^\circ$ at the subendocardium to -60° at the subepicardium, although a large variation be-

tween measurements exists. Data on the transverse angle are incomplete, stating only that it is typically on the order of a few degrees, being positive near the base and negative near the apex (23, 25).

According to mathematical models of cardiac wall mechanics, the distribution of myofiber orientation within the cardiac wall is the main determinant of the distribution of stress and myofiber shortening throughout the wall during ejection (1, 2, 5, 7). Small variations in the fiber orientation within the range of the reported values ($\pm 10^\circ$) resulted in large variations ($\pm 50\%$) of calculated myofiber stress (5). Therefore, it was concluded that the accuracy of the present methods to quantify fiber orientation was not sufficient to estimate local myofiber load.

Accuracy of measured myofiber orientation data is limited by several causes. Partly, the lack of accuracy can be attributed to the employed histological technique. Although in a well-cut slice the in-plane fiber orientation can be measured accurately, the possible out-of-plane component remains unknown. This severely affects the accuracy with which the transverse angle can be measured. Typically, the resulting accuracy of histological techniques is limited to $\sim 10^\circ$ (19, 26), and the best volume resolution obtained is $\sim 10 \text{ mm}^3$ (14).

Another issue in the quantitative description of the fiber orientation is the ambiguity in the definition of a local wall-bound coordinate system. Irregularities in the shape of the cardiac wall, such as the presence of papillary muscles and trabeculations at the endocardial wall, hamper the definition of a local coordinate system.

The purpose of this study was to more accurately assess three-dimensional cardiac myofiber orientation by applying magnetic resonance (MR)-diffusion tensor imaging (MR-DTI) and a novel definition of the local coordinate system.

MR-DTI has been developed to measure the diffusion tensor for water in biological tissues (3, 4). In validation studies performed in muscular tissues, it has been

Address for reprint requests and other correspondence: P. Bovendeerd, Dept. of Biomedical Engineering, Eindhoven Univ. of Technology, PO Box 513, 5600 MB Eindhoven, The Netherlands (E-mail: p.h.m.bovendeerd@tue.nl).

The costs of publication of this article were defrayed in part by the payment of page charges. The article must therefore be hereby marked "advertisement" in accordance with 18 U.S.C. Section 1734 solely to indicate this fact.

shown that the principal direction of the diffusion tensor corresponding to the largest diffusivity is statistically similar to the myofiber direction (10, 11, 20, 28). Also, the technique has been used to reconstruct the fiber orientation in one rabbit heart (21) and a human heart in vivo at low resolution (16, 27). However, quantitative results have not been reported. Compared with histological methods, the main advantage of MR-DTI is that true three-dimensional myofiber direction vectors are determined in the intact heart with respect to the well determined magnet coordinate system.

To obtain an unambiguous definition of the local coordinate system, it was investigated whether such a coordinate system could be defined based on the characteristics of the myofiber field.

Therefore, myofiber orientation was measured and quantified by the transmural course of the helix angle and the apex-to-base course of the midwall transverse angle using a novel definition of the local coordinate system. Fiber orientation between several normal hearts was compared.

Furthermore, we evaluated the divergence of the myofiber orientation field, which was suggested to be close to zero in a study by Peskin et al. (15). The divergence value may be elevated in regions where irregularities in the cardiac fiber field occur, such as the attachment of the right ventricle (RV) and the papillary muscles.

METHODS

This study was performed on five healthy female goats weighing 26–55 kg that were killed for unrelated orthopedic experiments. After an overdose of Euthasate, the goats were bled to death. The chest was opened and the heart was rapidly excised and rinsed in cold saline. After the removal of the atria, the ventricles were weighed. Thereafter, the heart was casted in a 20% gelatin substance to maintain its shape and subsequently stored at 4°C. Before measurement, the samples were allowed to adjust to a room temperature of 20°C. MR-DTI measurements were performed within 3 days.

Diffusion tensor imaging. ^1H MR-DTI measurements were performed in a 4.7-T magnet interfaced to a Varian NMR spectrometer. The instrument was equipped with a gradient insert (inner diameter 12 cm) that provided a maximal gradient strength of 220 mT/m with a rise time of 500 μs . Bore temperature was maintained at 20°C. The gelatin-casted heart was wrapped in plastic foil and placed in a birdcage radiofrequency coil in the center of the magnet. The long axis of the left ventricle (LV) was visually aligned with the center line of the magnet bore. Diffusion-weighted images were collected with a pulsed field gradient, spin-echo MRI sequence (22), in which the dephasing lobe of the read-out gradient was applied immediately before the data acquisition window to minimize cross talk between the imaging gradients and the diffusion-sensitizing gradients (13). Diffusion weighting was provided using a pair of unipolar rectangular gradient pulses with a duration of $\delta = 15$ ms and a separation of $\Delta = 35$ ms. Echo time was 70 ms, and repetition time was 4 s. Diffusion data were measured in 3-mm-thick adjoining slices. The number of slices varied with heart size and was between 19 and 25. The field of view of 100×100 mm and was represented with an image of 128×128 pixels, resulting in a pixel size of 0.78×0.78 mm². Diffusion gradients were applied in 10 directions, optimized according to Jones et al.

(12). For each direction, two different magnitudes of the sensitizing gradient were applied. The strength of these gradients was optimized according to Jones et al. (12), which implies that one measurement with minimal diffusion weighting was followed by another measurement in which $\sim 66\%$ of the signal vanished. In our experiments, Jones' condition was met with b values, as defined by others (8), of 0 and 1,763 s/mm². Two averages were acquired in a total measurement time of ~ 2.5 h.

Determination of the myofiber direction. For each diffusion direction, apparent diffusion coefficients (ADCs) were determined in each pixel. The 10 ADC maps thus derived were used to calculate the tensor components of the diffusion tensor in a least-squares approach. Because ADC values typically range from 0.1×10^{-3} to 2.2×10^{-3} mm²/s, the latter value being the diffusivity measured in free water, ADC values outside this interval were considered unrealistic and were excluded from further analysis. The eigenvector corresponding to the largest eigenvalue of the diffusion tensor was considered to be the myofiber orientation, quantified with respect to the magnet coordinate system. The reliability of the calculated myofiber orientation was assessed by the degree of anisotropy of the diffusion tensor, as quantified by the fractional anisotropy (FA), as introduced by Basser et al. (4). The FA value indicates the fraction of the diffusion that may be attributed to anisotropic diffusion.

Determination of an anatomic coordinate system. To quantify fiber orientation in terms of the commonly used helix and transverse angle, a transformation from the global magnet coordinate system to the anatomic coordinate system of the heart was performed (Fig. 1). The normal to the imaging plane was taken as a first estimate of the local long-axis direction. In each slice, the pixels corresponding to myofibers with an out-of-plane component smaller than $\pm 0.1 \pi$ -rad ($\sim 5.7^\circ$) were selected as a first estimate of the midwall region. A best fit circle through these pixels was calculated, yielding a first estimate of the center of the LV in that slice. Next, the local long-axis direction was then determined as the best fit line through the centers of the LV cross sections in five adjoining slices. The local myofiber orientation was reevaluated with respect to the new estimate of the local long-axis direction. Thus a new set of midwall myofiber pixels was found. Again, a circle was fitted to these pixels to yield the true LV center in a slice. This center served as the origin of a local cylindrical coordinate system along the local anatomic long axis. The direction with angle $\Phi = 0$ was defined

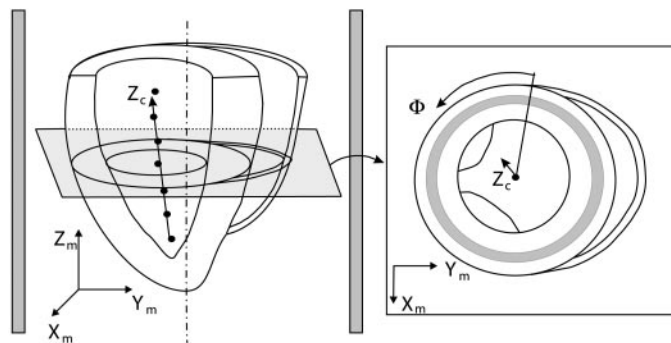


Fig. 1. Definition of the local cylindrical coordinate system (R , Φ , Z_c) relative to the rectangular magnet coordinate system (X_m , Y_m , Z_m). The axis Z_c is aligned with the centers of the nearby short-axis cross sections. The angle $\Phi = 0$ indicates the anterior connection of the right ventricular (RV) free wall to the left ventricle (LV). *Right*: pixels corresponding to myofibers with an out-of-plane component smaller than $\pm 0.1 \pi$ -rad are indicated by the gray area.

along the anterior RV fusion site. Thus the image plane may be tilted in the local cylindrical coordinate system.

Presentation of fiber direction data. For each goat heart, fiber orientations were measured in 50,000 voxels typically. Because it is impossible to show all data, a selection was made to illustrate the main characteristics of the fiber field. The helix angle was evaluated at several sectors in the equatorial LV short-axis slice. The transverse angle was determined in the midmyocardial free wall for all slices from apex to base and averaged over the circumference. Furthermore, the divergence of the fiber field was calculated at each voxel.

Selection of the equatorial slice. The equatorial slice was defined as the slice that was positioned at one-third of the long-axis length from the base of the heart (26). The base of the heart was defined as the slice nearest to the outflow tract but not showing it. The apex was the first slice showing cardiac tissue.

Helix angle. The definition of the fiber direction is ambiguous, because flipping the fiber direction by 180° results in the same fiber direction. Therefore, the vector defining fiber orientation was selected such that the circumferential component was always positive. The helix angle (α_h^*) was calculated as the angle between the myofiber direction and the plane perpendicular to the local long-axis direction (Fig. 2). The transmural course of the helix angle was determined for anterior, interpapillary muscle, posterior, and septal sectors, each sector being 20° wide (Fig. 3). The radius at which the helix angle changes sign [$R_0(\Phi)$] was determined for each region using a fifth-order polynomial fit through the data. This radius was used to normalize the transmural position (R)

$$h = \frac{R - R_0}{R_0} \tag{1}$$

where h is the normalized transmural coordinate. For all sectors in each heart, the slope of the transmural course of the helix angle was determined using a linear fit to the transmural data for the compact portion of the wall, defined as $h > -0.3$. To characterize the average helix angle course of all five hearts, helix angle data were grouped and a polynomial fit was determined in all four sectors. The papillary muscles were excluded based on visual inspection, and the endocardial radius was determined. The normalized endocardial position (h_{endo}) could then be calculated using the above-mentioned equation.

Midwall transverse angle. The transverse angle is the angle by which the cardiac myofibers cross the wall from the epicardium to endocardium. α_t^* was defined as the angle

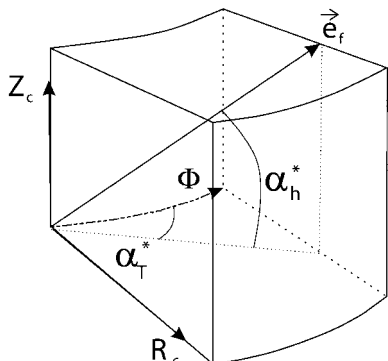


Fig. 2. Block of cardiac tissue as taken from the wall to show definition of helix angle α_h^* and transverse angle α_t^* . \vec{e}_r , Unit vector.

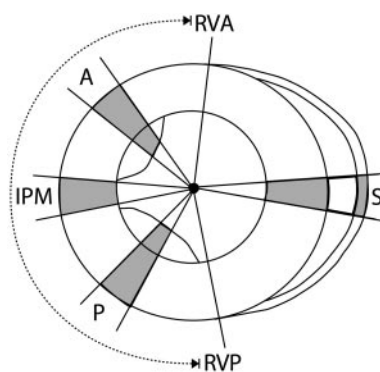


Fig. 3. LV sectors used for analysis of the helix angle data. A, anterior; IPM, interpapillary muscle; P, posterior; S, septum; RVA, anterior RV fusion site; RVP, posterior RV fusion site. The LV free wall is the region between the RVA and RVP, as indicated by the dotted line.

between the local circumferential direction and the projection of the fiber direction on the plane normal to the local long-axis direction (Fig. 2). In all slices, from apex to base, this angle was determined in the free wall at $R = R_0(\Phi)$, where the free wall is defined as the LV region spanned between the RV fusion sites (Fig. 3). The transverse angle was averaged over the circumference of the LV free wall. The apex-to-base length (L_{ab}) was scaled from 0 at the apex to 1 at the base.

Geometry. LV geometry was characterized by the mean radius at which the helix angle changes sign (R_m). This radius was determined in all slices from apex to base. L_{ab} was approximated by the distance between the basal and apical slice. Furthermore, the mean wall thickness of the equatorial slice (WT) was determined. For this analysis, the papillary muscles were excluded.

Statistical analysis. To investigate whether the ranges and slopes of the transmural helix angles were different in the different sectors, a multiple-sample comparison was performed. An ANOVA table was constructed, and a F -test was performed to evaluate whether there was a statistically significant difference between the means of the variables at the 95% confidence level. If so, a multiple-range test was performed using Fisher's least-significant difference procedure to assess which mean values were mutually significantly different. The order of the polynomial fits applied to the data was determined using an ANOVA analysis for the coefficients of the polynomial in the order fitted.

Divergence of the fiber field. Peskin (15) showed that from the quasistatic momentum equilibrium equations, it can be derived that the divergence of the cardiac fiber field is zero using the following assumptions: 1) during ejection, active stress is the most important determinant of cardiac stress; 2) active stresses are mainly uniaxial; 3) myofiber stress distribution is uniform throughout the wall; and 4) the hydrostatic pressure gradient is oriented perpendicular to the fiber direction. To investigate to which extent these assumptions hold in the real heart, we computed the magnitude of the divergence of the fiber field on a pixel-by-pixel basis as Eq. 2.

We described the fiber field by unit vector \vec{e}_f , where $[u, v, w]$ represents the components with respect to the $[x, y, z]$ magnet coordinate system. The magnitude of the divergence (MD) of the fiber field was defined as follows

$$\text{MD} = \left| \vec{\nabla} \cdot \vec{e}_f \right| = \left| \frac{\partial u}{\partial x} + \frac{\partial v}{\partial y} + \frac{\partial w}{\partial z} \right| \tag{2}$$

Table 1. *Most important global properties of the heart*

	R_m , mm	L_{ab} , mm	L_{ab}/R_m	M , g	WT, mm
Heart 1	17.04	54	3.17	89.0	10.27
Heart 2	17.09	54	3.17	97.5	11.60
Heart 3	16.23	51	3.14	94.5	10.12
Heart 4	20.77	69	3.32	185.0	12.84
Heart 5	21.27	69	3.24	180.0	12.65
Mean	18.5	59.4	3.20	129.2	11.5
SD	2.4	8.9	0.07	48.8	1.3

R_m , left ventricular radius at the equator; L_{ab} , apex-to-base length; M , mass of the ventricles; WT, mean wall thickness of the equatorial slice. The ratio of L_{ab} to R_m characterizes heart shape.

The divergence of the fiber field can be interpreted as a measure of structural continuity of the myofiber field. The requirement that the divergence of the fiber field is zero is the translation of the assumption that the cross-sectional area of a fiber remains constant (15). In other words, every myofiber that enters a voxel must also leave this voxel again.

RESULTS

General geometric characteristics of the hearts are summarized in Table 1. Total LV and RV mass of the ventricles was 129.2 ± 48.8 g (mean \pm SD). R_m and L_{ab} of the LVs were 18.5 ± 2.4 and 59.4 ± 8.9 mm, respectively.

The out-of-plane component of the fiber orientation in the equatorial plane as well as the projection of the fiber orientation onto the plane are shown in Fig. 4. More axially oriented fibers are found near the epicardium and endocardium and in the papillary muscles. Midwall fibers run predominantly in the circumferential direction. At the posterior RV fusion site, there is a smooth transition of in-plane fibers from the LV to the RV. At the anterior RV fusion site, this transition is more abrupt.

The transmural course of the helix angle, as shown in Fig. 5, typically ranges from $+90$ to -75° at the anterior site, from $+85$ to -55° at the intrapapillary muscle site, from $+80$ to -40° at the posterior site, and from $+50$ to -85° at the septal site.

The range of the helix angles was largest in the anterior sector and significantly smaller in the posterior sector (Table 2). The slope of transmural course of the helix angles was steeper in the anterior and septal sectors than in posterior and interpapillary muscle sectors. In all sectors except for the septal sector, a contribution of the papillary muscles was visible as a plateau of 90° fibers. In the subepicardial layers of the anterior and septal sectors, a steep slope was observed.

The papillary muscles were excluded from the data to allow comparison with standard normalization techniques. Consecutively, transmural helix angle data of all five hearts were grouped and fitted using a fifth-order polynomial, which resulted in an optimum fit in view of model complexity and statistical significance of the coefficients. The SD in myofiber orientation thus observed was on the order of $\pm 6^\circ$ in all sectors (Fig. 5).

The transverse angle varies from apex to base as shown in Fig. 6. With the use of a third-order poly-

mial fit to the data, the mean transverse angle course varied from $-12 \pm 4^\circ$ near the apex to $+9 \pm 4^\circ$ near the base of the heart. The change of sign of the transverse angle occurred between the equator and base of the heart. The apex-to-base course of R_m (Fig. 6) was best described by an elliptical course. The mean equatorial radius appeared to be 19 mm.

The divergence of the myofiber field was <0.07 mm^{-1} in the major part of the myocardial walls but significantly exceeded this level at the anterior fusion of the RV and LV walls and at the insertion sites of the papillary muscles (Fig. 7).

DISCUSSION

DTI measurements. Fiber orientation was measured postmortem in five goat hearts using MR-DTI. Less than 2% of the ADC values were excluded from the data. Values for the FA as found in the literature for fresh myocardial tissue range from 0.17 to 0.65 (8, 11, 16). Our value of 0.35 ± 0.03 is well within this range, indicating that the fiber direction was well determined. Most MR-DTI measurements were performed within 4 h after excision of the heart. We compared the FA values of hearts that were measured immediately after excision and those that were measured after 3 days. The FA values appeared not to be significantly different between both groups, implying that the structures that are responsible for the diffusion anisotropy are still intact 3 days after excision.

Typically, in one heart, fiber orientation was measured in $\sim 50,000$ voxels with a voxel size of 1.8 mm^3 , which is an enhancement in volume resolution compared with histological measurement techniques by a factor of 5. Regionally, the long-axis direction was defined by the direction of a line through center points of the LV in the nearby slices. The transmural coordinate was normalized unambiguously using R_0 . Myofiber orientations have been characterized by the helix and transverse angles. SDs for helix angles measured in individual hearts were in the order of $\pm 6^\circ$, which is slightly less than the $\pm 10^\circ$ obtained in histological measurements.

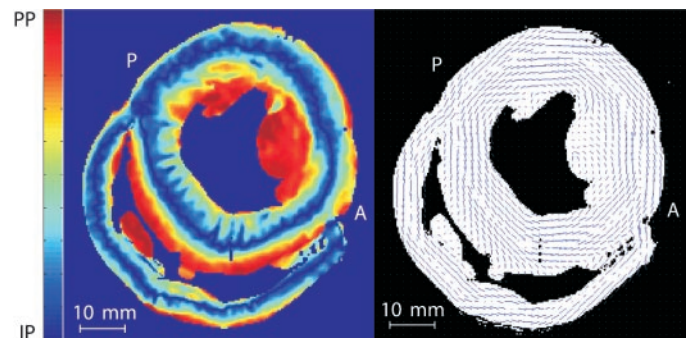
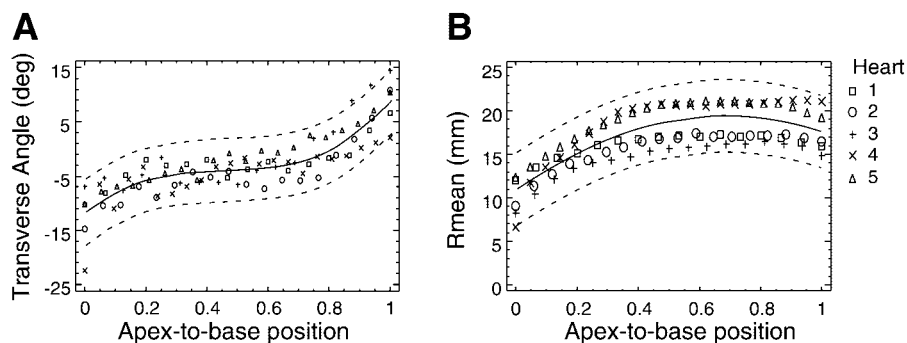


Fig. 4. Visualization of the cardiac fiber field in an equatorial slice. *Left*: out-of-plane component of the fiber direction. Blue colors indicate the in-plane (IP) fiber direction; red colors indicate fiber direction perpendicular to the plane (PP). *Right*: projection of the fiber direction onto the imaging plane. P and A indicate the posterior and anterior LV free wall, respectively.

Fig. 6. A: transverse angle course from apex to base. B: mean radius at which the helix angle changes sign (R_m) as a function of the apex-to-base position. Solid lines indicate average course; dashed lines indicate 95% confidence intervals for predicted values.



3, where β now represents the misalignment error. This implies that for misalignment errors in the order of $\pm 10^\circ$, the error in the transverse angle is as little as $\sim 2\%$ of the calculated α_t^* .

Normalized transmural position. Usually the transmural position is normalized to the local wall thickness. However, determination of wall thickness is difficult due to the presence of papillary muscles and endocardial trabeculations, which hampers detection of the endocardial wall (19, 26). Instead of normalization using the endocardial wall, R_0 is much better defined and has a smooth appearance. Therefore, R_0 was used as a reference radius to which all transmural distances were normalized in this study. Recognition of common patterns between different hearts is therefore enhanced using this normalization technique.

To compare our normalization method with the commonly used method, the transmural course of the fiber orientation normalized between endocardium and epi-

cardium was also calculated. The endocardial wall was determined from the divergence plots, where the papillary muscles could be detected. The SD to the helix angle data determined in this manner appeared to be 11° , which is considerably more than the 6° found using our normalization method.

Helix and transverse angle data. Our data on the helix angle are within the range of earlier reported measurements and model predictions (1, 9, 14, 17, 19, 23, 24, 26).

To our best knowledge, these are the first detailed measurements of the transmural component of muscle fiber direction as a function of the longitudinal position. Earlier studies reported values at only a few longitudinal positions, often averaged across the wall thickness. For comparison with these data, we assume a parabolic transmural course of the transverse angle, with a zero angle at the endocardium and epicardium. Our midwall value then equals 1.5 times the transmural average value. Near the apex, the average transmural angle was measured to be -4.5° (23), which is lower than our averaged value of -7.8° . Halfway between the apex and equator, literature (23) and our values are similar, equaling -3.5 and -3° , respectively. Averaged over the subequatorial region, a midwall value of -8.0° has been reported (25), which compares reasonably with our value of -6° . Averaged throughout the whole heart, we obtained a value of -3° , which is considerably lower than the value of -7.9° obtained by Scollan et al. (20, 21). This may be because in our analysis the most apical slices were left out because determination of the long axis was considered to be inaccurate. In the apical slices, however, the highest values for the transverse angle are expected. Finally, the transverse angle course that we measured compares well to the optimization prediction by Rijcken et al. (6, 18).

It has been assumed that myofiber orientation adapts such that local stresses and strains are distributed uniformly throughout the heart (15, 17, 18). Employing this condition in a mathematical model, fiber orientation can be optimized to obtain homogeneous fiber shortening during ejection (18). The resulting optimum orientation was found to be well determined, indicating that variation of fiber orientation in between hearts may be small. This finding was confirmed by the present study.

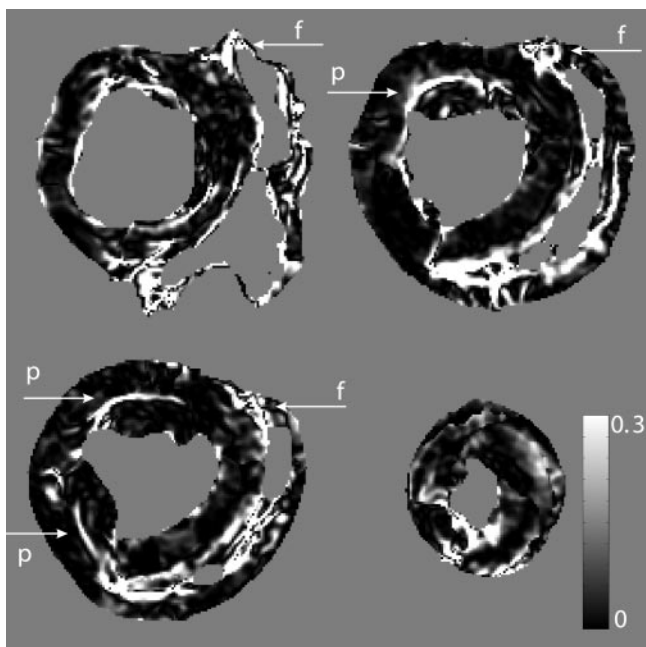


Fig. 7. Divergence plots in which black indicates low divergence values and white indicates divergence $> 0.3 \text{ mm}^{-1}$. Top left: basal slice; top right: equatorial slice; bottom left: slice in middle between apex and equator; bottom right: apical slice. Arrows indicate the papillary muscle (p) and RV fusion (f) regions, where the divergence values are significantly higher than 0.08 mm^{-1} .

Divergence of the fiber field. As shown by Peskin (15), the assumption that tissue loads are mainly transmitted by the active fibers, each fiber bearing the same load, can be converted to the condition that the divergence of the fiber field is zero. In our study, the divergence of the fiber field was $<0.07 \text{ mm}^{-1}$ throughout the myocardium and significantly elevated at the insertion sites of the papillary muscles and at the anterior RV fusion site. Thus calculation of the divergence may enable detection of papillary muscle structures.

However, we found that it was not possible to evaluate stress uniformity on the basis of our measurements, because it can be shown that an active stress inhomogeneity of 10% results in a divergence value of $\sim 0.005 \text{ mm}^{-1}$. To detect these small differences, an accuracy of $\sim 0.3^\circ$ is necessary, which greatly exceeds the current 6° accuracy.

In conclusion, the myofiber structure offers an excellent base for the definition of a cardiac coordinate system, based on the local long-axis direction and the transmural coordinate normalized using R_0 . With respect to this coordinate system, helix and transverse angles can be defined to characterize the fiber field.

The transmural course of the helix angle we found compares well to earlier measurements. The slope of the transmural helix angle course is largest at the anterior and septal sites. The apex-to-base course of the transverse angle varies according to a third-order polynomial, with values of -12° at the apex and $+9^\circ$ at the base.

Both the transmural course of the helix angle and the apex-to-base course of the transverse angle that we measured corresponded well to model predictions based on uniformity of stress and strain.

The divergence of the myofiber field appeared to be $<0.07 \text{ mm}^{-1}$ in the major part of the myocardial walls except for sharp transitions at the fusion sites between the LV and RV and at the insertion of the papillary muscles. The accuracy with which the measurements were performed is not good enough to allow evaluation of uniformity of the stresses.

The authors gratefully acknowledge the technical assistance of Hans Vosmeer and Boudewijn van der Sande.

REFERENCES

- Arts T, Prinzen FW, Snoeckx LHEH, Rijcken JM, and Reneman RS. Adaptation of cardiac structure by mechanical feedback in the environment of the cell: a model study. *Biophys J* 66: 953–961, 1994.
- Arts T, Veenstra PC, and Reneman RS. A model of the mechanics of the left ventricle. *Ann Biomed Eng* 7: 299–318, 1979.
- Basser PJ, Mattiello J, and LeBihan D. MR diffusion tensor spectroscopy and imaging. *Biophys J* 66: 259–267, 1994.
- Basser PJ and Pierpaoli C. Microstructural and physiological features of tissues elucidated by quantitative-diffusion-tensor MRI. *J Magn Reson* 111: 209–219, 1996.
- Bovendeerd PHM, Arts T, Huyghe JM, van Campen DH, and Reneman RS. Dependence of local left ventricular wall mechanics on myocardial fiber orientation: a model study. *J Biomech* 25: 1129–1140, 1992.
- Bovendeerd PHM, Rijcken J, van Campen DH, Schoofs AJG, Nicolay K, and Arts T. Optimization of left ventricular muscle fiber orientation. In: *Proc IUTAM Symposium on Synthesis on Bio Solid Mechanics*, edited by Pedersen P and Bendsøe P. Copenhagen, Denmark: 1998, p. 285–295.
- Chadwick RS. Mechanics of the left ventricle. *Biophys J* 39: 279–288, 1982.
- Garrido L, Wedeen VJ, Kwong KK, Spencer UM, and Kantor HL. Anisotropy of water diffusion in the myocardium of the rat. *Circ Res* 74: 789–793, 1994.
- Greenbaum RA, Yen Ho S, Gibson DG, Becker AE, and Anderson RH. Left ventricular fibre architecture in man. *Br Heart J* 45: 248–263, 1981.
- Hsu EW, Muzikant AL, Matulevicius SA, Penland RC, and Henriques CS. Magnetic resonance myocardial fiber-orientation mapping with direct histological correlation. *Am J Physiol Heart Circ Physiol* 274: H1627–H1634, 1998.
- Holmes JW, Scollan DF, and Winslow RL. Direct histological validation of diffusion tensor MRI in formaldehyde-fixed myocardium. *Magn Reson Med* 44: 157–161, 2000.
- Jones DK, Horsfield MA, and Simmons A. Optimal strategies for measuring diffusion in anisotropic systems by magnetic resonance imaging. *Magn Reson Med* 42: 515–525, 1999.
- LeBihan D. Molecular diffusion NMR imaging. *Magn Res* 7: 1–30, 1991.
- Nielsen PMF, LeGrice IJ, Smail BH, and Hunter PJ. Mathematical model of geometry and fibrous structure of the heart. *Am J Physiol Heart Circ Physiol* 260: H1365–H1378, 1991.
- Peskin CS. Fiber architecture of the left ventricular wall: an asymptotic analysis. *Commun Pure Appl Math* 42: 79–113, 1989.
- Reese TG, Weisskoff RM, Smith RN, Rosen BR, Dinsmore RE, and Wedeen VJ. Imaging myocardial fiber architecture in vivo with magnetic resonance. *Magn Reson Med* 34: 786–791, 1995.
- Rijcken J, Bovendeerd PHM, Schoofs AJG, van Campen DH, and Arts T. Optimization of cardiac fiber orientation for homogeneous fiber strain at beginning of ejection. *J Biomech* 30: 1041–1049, 1997.
- Rijcken J, Bovendeerd PHM, Schoofs AJG, van Campen DH, and Arts T. Optimization of cardiac fiber orientation for homogeneous fiber strain during ejection. *Ann Biomed Eng* 27: 289–297, 1999.
- Ross MA and Streeter DD. Nonuniform subendocardial fiber orientation in the normal macaque left ventricle. *Eur J Cardiol* 3: 229–247, 1975.
- Scollan DF, Holmes A, Winslow R, and Forder J. Histological validation of myocardial microstructure obtained from diffusion tensor magnetic resonance imaging. *Am J Physiol Heart Circ Physiol* 275: H2308–H2318, 1998.
- Scollan DF, Holmes A, Zhang J, and Winslow R. Reconstruction of cardiac ventricular geometry and fiber orientation using magnetic resonance imaging. *Ann Biomed Eng* 28: 934–944, 2000.
- Stejskal EO and Tanner JE. Spin diffusion measurements: spin echoes in the presence of a time-dependent field gradient. *J Chem Phys* 42: 288–292, 1965.
- Streeter DD. Gross morphology and fiber geometry of the heart. In: *Handbook of Physiology. The Cardiovascular System. The Heart*. Bethesda, MD: Am. Physiol. Soc., 1979, sect. 2, vol. I, chapt. 4, p. 61–112.
- Streeter DD and Hanna WT. Engineering mechanics for successive states in canine left ventricular myocardium. II. Fiber angle and sarcomere length. *Circ Res* 33: 656–664, 1973.
- Streeter DD, Powers WE, Ross MA, and Torrent-Guasp F. Three-dimensional fiber orientation in the mammalian left ventricular wall. In: *Cardiovascular System Dynamics*, edited by Baan H, Noordergraaf A, and Raines J. Cambridge, MA: MIT Press, 1978, p. 73–78.
- Streeter DD, Spotnitz HM, Patel DP, Ross J, and Sonnenblick EH. Fiber orientation in the canine left ventricle during diastole and systole. *Circ Res* 24: 339–347, 1969.
- Tseng WYI, Reese TG, Weisskoff RM, and Wedeen VJ. Cardiac diffusion tensor MRI in vivo without strain correction. *Magn Reson Med* 42: 393–403, 1999.
- Van Donkelaar CC, Kretzers LJG, Bovendeerd PHM, Lataster LMA, Nicolay K, Janssen JD, and Drost MR. Diffusion tensor imaging in biomechanical studies of skeletal muscle function. *J Anat* 194: 79–88, 1999.